

Gradient transport processes in $E \times B$ plasmas

Cliff A. Thomas* and Mark A. Cappelli†
 Stanford University, Stanford, CA, 94305-3032

Various classes of non-quiet magnetized plasma exhibit anomalous energy and/or momentum diffusivity. In this case, ‘anomalous’ is meant to characterize a transport regime wherein the measured property flux disagrees with classical theory. In most examples anomalous transport is substantially higher than classical expressions predict; it is no different for the Hall accelerator. It has been well documented that the electron transport in a Hall accelerator can vary dramatically along its channel, and cannot be accounted for within an accepted physical framework. A myriad of justifications have been forwarded in an attempt to understand the cause of the observed transport, but all have fallen short - especially at low discharge voltage. When plasma fluctuations are considered to be the cause of anomalous transport, they are commonly suggested in the context of azimuthal fluctuations. Recent numerical calculations in an r-z hybrid code predict the existence of strong 2-5MHz axial oscillations best characterized by the dispersion relation for a beam-plasma instability. This paper reports on the instability, and forwards a saturation mechanism for longitudinal electrostatic oscillations considering gradient transport processes in the presence of an applied magnetic field. It is found that the nonlinear saturation of the observed instability is sufficient to explain the anomalous transport near the exit plane of the Hall accelerator.

Nomenclature

$U_{\zeta,m}$	=	velocity of species ζ , m direction
n_{ζ}	=	number density of species ζ
q_{ζ}	=	charge of species ζ
m_{ζ}	=	mass of species ζ
R	=	volumetric ionization rate
μ	=	mobility
ν	=	frequency
k	=	wave number
v	=	vector velocity
E	=	vector electric field
B	=	vector magnetic field
c	=	charge per unit mass
Ω_e	=	electron cyclotron frequency ($q_e B/m_e$)
Ω_e^*	=	effective electron cyclotron frequency
α	=	$E \times B$ shear factor
ν_e	=	electron-neutral collision frequency
V_{en}	=	electron drift due to electron-neutral collisions
V_{pd}	=	polarization drift
α_{max}	=	maximum alpha for a given electric field fluctuation
S	=	cyclotron orbit velocity
S^*	=	effective cyclotron orbit velocity
γ	=	angular phase of cyclotron orbit

* Research Assistant, Mechanical Engineering Department, MC 3032. Student Member, AIAA.

† Professor, Mechanical Engineering Department, MC 3032. Member, AIAA.

I. Introduction

ANOMALOUS transport is defined differently in certain circles, but is considered here in its most general definition: transport not explained by classical theory. Commonly, plasma confinement devices exhibit transport coefficients that scale as B^{-1} rather than B^{-2} , a condition first noted by Bohm, Burhop, and Massey in 1946¹. The difference between the observed and predicted transport scaling coincided with unexpectedly poor magnetic confinement. The results portended future difficulties in plasma physics, and anomalous transport in magnetized plasma remains an impediment to the improved operation of many plasma confinement devices.

In the Hall accelerator, ion acceleration is sought between an anode and a hot-emitting cathode. To maximize the ion current fraction and increase device efficiency, electron motion is impeded by a magnetic field normal to the current conduction path². Unfortunately, the current isn't completely carried by ions, as electrons leak through the magnetic field at a rate unexplained by classical, neoclassical, or Bohm diffusion parameters²⁻⁴. In fact, experiments show that the electron mobility varies dramatically throughout the channel, and in different regions exhibits values reminiscent of *each* of the aforementioned transport regimes. This makes the Hall accelerator a challenging device to self-consistently model, but a remarkable device for studies pertaining to the cause and mitigation of various anomalous transport mechanisms.

A variety of theories have been forwarded to explain the transport near the exit plane of the Hall accelerator, but none have found full community acceptance. Recent numerical calculations in a r-z hybrid code predict strong 2-5MHz axial oscillations in this region. MHz oscillations have been reported in experiment^{5,7}. Thoughts on anomalous transport have usually considered fluctuations in an azimuthal context^{5,7}, but the recent finding motivates a reconsideration of the possible role of axial instabilities. The observed axial fluctuations represent a beam-plasma parametric instability with an unresolved azimuthal component. To better understand the impact of this instability on transport, a saturation mechanism for longitudinal electrostatic oscillations in an applied magnetic field is derived considering gradient transport processes in space and time. With this result, the nonlinear saturation of the observed instability is found to be sufficient explanation for the anomalous transport near the exit plane of the Hall accelerator.

II. Beam-plasma parametric instability

The r-z hybrid code in question is designed to simulate the Stanford SPT. The code's primary input parameters are the position dependent electron mobility (determined by experiment), the electron-wall secondary emission coefficient, and an electron-wall damping coefficient. As per previous publications regarding this r-z code, the electric field, ion acceleration curve, and electron temperature are accurately captured when the experimentally measured mobility is employed⁸.

Figure 1 displays the power spectral density of electric field fluctuations in the r-z hybrid code. The power spectral density is evaluated at the accelerator's center radius. Strong fluctuations are observed, and transit time oscillations from 200-500kHz are prominent. Instabilities in this range are witnessed in separate numerical efforts⁹. A summary of the instabilities observed through 200kHz is available in published literature¹⁰. New features are reported at 2-5MHz, as more comprehensive analysis has lifted the earlier studies' Nyquist limit. Instabilities in this frequency band have been evidenced in the Stanford SPT⁶, and observed in many high frequency investigations at a variety of disparate operating conditions^{5,7}.

It is important to note that it is difficult at this stage to definitively assert whether the observed instability is real due to limitations in the hybrid code. Even if it is, it is impossible at this time to determine whether discrete effects are aggravating or damping the instability. Regardless, the instability is considered to be intriguing for further investigation based on: (a) that the instability has not been found to correspond to any known numerical disturbance,

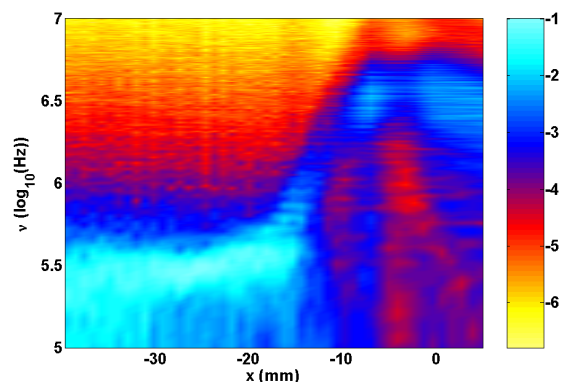


Figure 1. Power spectral density normalized by axial position, in log scale, of the R-Z Hybrid code's electric field fluctuations.

(b) is limited to the acceleration region, (c) exists in a frequency band readily observed in experiments, and (d), is found to correspond to a readily derived dispersion relation corresponding to an beam-plasma instability, as described below.

The beam-plasma dispersion relation is evaluated using perturbation theory. The mass and momentum conservation equations are summarized in Eqs.(1) through (4) below.

$$\frac{dn_i}{dt} + \frac{d}{dx} (n_i U_{i,x}) = R \quad (1)$$

$$\frac{dn_e}{dt} + \frac{d}{dx} (n_e U_{e,x}) = R \quad (2)$$

$$\frac{dU_{i,x}}{dt} + U_{i,x} \frac{dU_{i,x}}{dx} = \frac{q_i}{m_i} E_x - R U_{i,x} \quad (3)$$

$$U_{e,x} = \mu E_x \quad (4)$$

The velocity, number density, and electric field are assumed to obey conventional forms.

$$U_{i,x} = U_{io}(x) + \tilde{U}_i e^{j(kx - \omega t)} \quad (5)$$

$$U_{e,x} = U_{eo}(x) + \tilde{U}_e e^{j(kx - \omega t)} \quad (6)$$

$$n_i = n_{io}(x) + \tilde{n}_i e^{j(kx - \omega t)} \quad (7)$$

$$n_e = n_{eo}(x) + \tilde{n}_e e^{j(kx - \omega t)} \quad (8)$$

$$E_x = E_o(x) + \tilde{E} e^{j(kx - \omega t)} \quad (9)$$

The electron and ion conservation equations are coupled at relatively low k and ω via quasi-neutrality.

$$\tilde{n}_e = \tilde{n}_i \quad (10)$$

The dispersion relation is then given by Eq. (11) through (16).

$$a_4 = U_{io}^2 \quad (11)$$

$$a_3 = -2\omega U_{io} \quad (12)$$

$$a_2 = -2U_{io} \frac{dU_{io}}{dx} + \frac{eE_o}{M_i} \quad (13)$$

$$a_1 = \omega^2 + R^2 - \left(\frac{dU_{io}}{dx} \right)^2 + \frac{e}{\mu m_i} \left(\frac{dU_{eo}}{dx} - R \right) \quad (14)$$

$$a_0 = 2\omega \frac{dU_{io}}{dx} - \frac{e\omega}{\mu m_i} \quad (15)$$

$$a_4 k^2 + (a_3 + a_2 j)k + (a_1 + a_0 j) = 0 \quad (16)$$

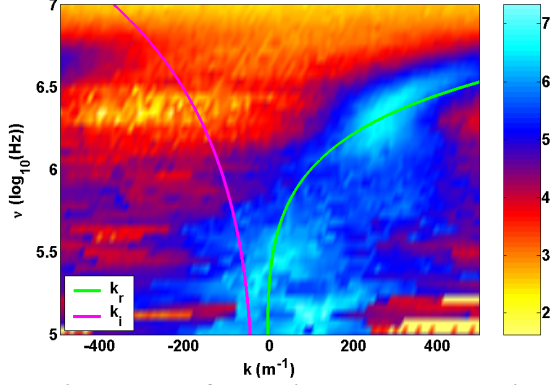


Figure 2. The k-w fluctuation power, normalized by power at a given frequency, plotted against the beam-plasma dispersion relation. $x = -10\text{mm}$, $U_i = 4700\text{m/s}$.

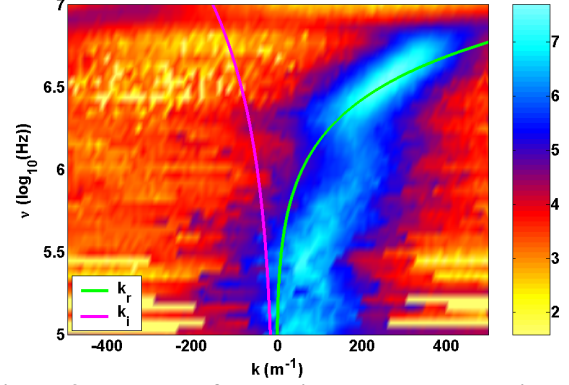


Figure 3. The k-w fluctuation power, normalized by power at a given frequency, plotted against the beam-plasma dispersion relation. $x = -5\text{mm}$, $U_i = 9500\text{m/s}$.

For a 200V discharge in the r-z hybrid code, one finds that there is an unstable solution to Eq. (16) near the exit plane. In the r-z simulation, it is expected that energy from streaming ions is converted into fluctuation energy. The fluctuations will serve to thermalize the ion beam and further contribute to electron transport. It is also possible the instability could be enhanced by interactions with the simulation's constant potential boundary conditions, as found for transit time instabilities in other studies¹¹. Because the code is r-z geometry, the instability may have an unresolved azimuthal component.

Support for the presence of the beam-plasma instability at 2-5MHz is provided in Fig. (2) and Fig. (3). The k-w fluctuation power predicted by the hybrid simulation is plotted, normalized by power at a given frequency, and drawn in logarithmic scale. The unstable solution to Eq. (16) is also visible in these figures. Two separate locations near the exit plane are shown, and the beam-plasma dispersion relation is found to explain the strong 2-5MHz oscillation for axial wave numbers greater than 200m^{-1} . Because the code is unable to resolve wave numbers greater than 500m^{-1} , extrapolation to higher frequencies is uncertain, but it is reasonable to assume the instability would display some prominence at higher frequencies in the absence of discrete limitations.

As a final note for this section, it is interesting that the phase velocity of the unstable root is comparable to that of the fast transit time instability near the exit. This suggests that the beam-plasma parametric instability detailed here can be considered a high frequency manifestation of the general transit time instability. In this case, the ion beam velocity is sufficient to induce plasma instability in the absence of other aggravating factors.

III. Saturation of Longitudinal Oscillations

The classical solution of the Boltzmann transport equation in magnetized plasma neglects spatially varying electric fields, a phenomenon associated with fluctuations and plasma non-neutrality. This oversight becomes important in 1-D for plasma with constant magnetic field when the spatial gradient of the classical drift velocity is comparable to the cyclotron frequency. The mobility in this scenario can be substantially modified. This can be understood by considering the trajectory of a charged particle subject to the Lorentz force equation; the particle's charge per unit mass is equal to c .

$$\frac{d\vec{v}}{dt} = c\vec{E} + c\vec{v} \times \vec{B} \quad (17)$$

If the magnetic field is constant, taking the first temporal derivative of Eq. (17) yields Eq. (18).

$$\frac{d^2\vec{v}}{dt^2} = c\frac{d\vec{E}}{dt} + c\frac{d\vec{v}}{dt} \times \vec{B} \quad (18)$$

Substituting Eq. (17) into Eq. (18) results in Eq. (19), where the velocity is considered in the plane perpendicular to the magnetic field.

$$\frac{d^2\vec{v}}{dt^2} + \Omega_e^2\vec{v} = c \frac{d\vec{E}}{dt} + c^2\vec{E} \times \vec{B} \quad (19)$$

Equation (19) allows for classical charged particle motion if the electric field is a function of time only; this includes harmonic cyclotron motion, cross-field drift, and polarization drift. If the electric field is a function of position as well, interesting consequences can develop. The first term on the right side of Eq. (19) is given by Eq. (20) (including spatial terms).

$$\frac{d\vec{E}(\vec{x}, t)}{dt} = \nabla_{\vec{x}}\vec{E}|_t \cdot \vec{v} + \frac{d\vec{E}}{dt}|_{\vec{x}} \quad (20)$$

Substituting Eq. (20) into Eq. (19) yields Eq. (21).

$$\frac{d^2\vec{v}}{dt^2} + \left(\Omega_e^2 I - c \nabla_{\vec{x}}\vec{E}|_t \right) \cdot \vec{v} = c \frac{d\vec{E}}{dt}|_{\vec{x}} + c^2\vec{E} \times \vec{B} \quad (21)$$

It is apparent that the classical trajectory of a charged particle is altered when the spatial gradient of the classical drift velocity is comparable to the cyclotron frequency. The effective cyclotron frequency is modified.

To see why Eq. (21) considers charged particle motion in fluctuating non-neutral plasma with constant magnetic field, it is only important to remember that in the local vicinity of a charged particle the electric field has spatial and temporal derivatives that manifest themselves through terms 3, 4, and 5 of Eq. (21), and that plasma non-neutrality expresses itself through electric field gradients. It is therefore obvious that in all non-quietest plasmas, the spatial and temporal nature of fluctuations can modify charged particle trajectories, and thereby modify charged particle mass, momentum, and energy transport.

If Eq. (21) is considered in a reference frame aligned with x , where x is parallel to the electric field gradient, and the frequency of fluctuations are much less than the cyclotron frequency, the solution to Eq. (21) can be cast in Eq. (22) through Eq. (27) for small Δt .

$$\alpha = \frac{dE}{dx} (B\Omega_e)^{-1} \quad (22)$$

$$\Omega_e^* = \Omega_e (1 - \alpha)^{1/2} \quad (23)$$

$$S^* = S (1 - \alpha)^{1/2} \quad (24)$$

$$\gamma = \Omega_e^* t - \phi \quad (25)$$

$$v_x = \frac{c \frac{dE_x}{dt}|_{\vec{x}}}{\Omega_e^{*2}} + \frac{c^2 (\vec{E} \times \vec{B})_x}{\Omega_e^{*2}} + S \cos(\gamma) \quad (26)$$

$$v_y = \frac{c \frac{dE_y}{dt}|_{\vec{x}}}{\Omega_e^{*2}} + \frac{c^2 (\vec{E} \times \vec{B})_y}{\Omega_e^{*2}} - S^* \sin(\gamma) \quad (27)$$

Equations (22) through (27) are striking as they indicate different confinement regimes based on the sign and magnitude of the electric field gradient in space. The effect of α has been documented¹², and is summarized here. For $\alpha < 0$ the effective cyclotron frequency is increased, the Larmor radii are tightened, and transport is decreased. When $0 < \alpha < 1$ the effective cyclotron frequency is decreased, the Larmor radii are larger, and transport is increased.

At $\alpha > 1$ the electric field gradient overcomes the magnetic field, and shear in the electric field demagnetizes the plasma.

To first order, the steady-state drift due to electron-neutral collisions is the classical expression modified by the effective cyclotron frequency, Ω_e^* .

$$V_{en} = \frac{\Omega_e \nu_e}{\nu_e^2 + \Omega_e^{*2}} \left(\frac{E}{B} \right) \quad (28)$$

Equation [28] can be expressed in a simpler form if $\Omega_e^* \gg \nu_e$.

$$V_{en} = \frac{\nu_e}{\Omega_e (1 - \alpha)} \left(\frac{E}{B} \right) \quad (29)$$

Perhaps even more important than the impact of α to steady-state drift though, is the impact of the effective cyclotron frequency to the classical polarization and $E \times B$ drifts. At this time the concentration will be on the polarization drift due to E_x , as E_y is unresolved in the R-Z code. This is unfortunate since azimuthal fluctuations are expected to contribute to electron transport^{1,5}, and may contribute substantially for axial/azimuthal instabilities that exhibit large values of α . If the fluctuation frequency is greater than the electron neutral collision frequency, the effect of the polarization drift can be pulled directly from Eq. (26).

$$V_{pd} = \frac{1}{\Omega_e (1 - \alpha)} \frac{d}{dt} \left(\frac{E}{B} \right) \quad (30)$$

Equation (29) and Eq. (30) can be combined to approximate the drift due to a strong electric field fluctuation normal to the magnetic field. Obviously, the net drift is substantially modified when α is large and the fluctuation frequency is \gg than the electron-neutral collision rate.

$$V_{en} + V_{pd} = \frac{1}{\Omega_e (1 - \alpha)} \left(\nu_e \left(\frac{E}{B} \right) + \frac{d}{dt} \left(\frac{E}{B} \right) \right) \quad (31)$$

Equation (31) can be solved on a time-average basis analytically for an electric field of the form given in Eq. (32). The solution is given by Eq. (33).

$$E_x(x, t) = E_o + \tilde{E} \sin(kx - \omega t) \quad (32)$$

$$\langle v_x \rangle = \frac{\nu_e}{\Omega_e} \frac{E}{B} + \left(\frac{\nu_e}{\Omega_e} \frac{E}{B} - \frac{\omega}{k} \right) \sum_{n=2,4,6}^{\infty} \frac{(n-1)!!}{(n)!} \alpha_{max}^n \quad (33)$$

Obviously, as the fluctuation intensity of an incident wave increases (as $\alpha_{max} \rightarrow 1$), the impact to transport is substantial. It is therefore surmised that as the parametric instability outlined in section II grows, it's intensity eventually approaches $\alpha_{max}=1$. As this happens though, the nonlinear response increases, and eventually the enhanced electron transport near $\alpha_{max}=1$ limits growth. The wave saturates.

To demonstrate the potential effect of fluctuations on transport, the electron momentum equation is solved for an electric field fluctuation of the form given in Eq. (32). Figure (4) and Fig. (5) display the solution for two cases. In Fig. (4), the magnitude of the electric field fluctuation is chosen to equal the average electric field. The wave number of the disturbance is also chosen to cause α_{max} near 1. In this case, anomalous transport is expected to make a substantial impact on the effective hall parameter. Figure (5) is calculated using a small fluctuation, so the net result is near-classical transport. The classical value of the hall parameter for both figures is 1000.

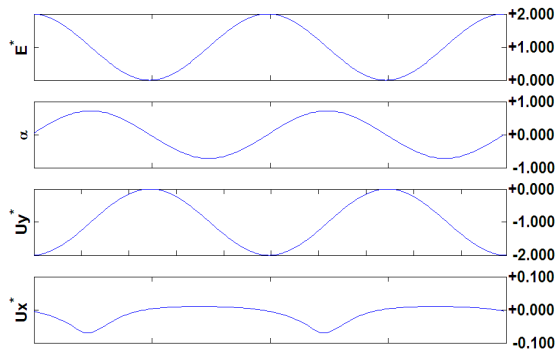


Figure 4. Electron momentum equation's solution for a prescribed electric field. $E_0 = 2000\text{V/m}$. $E_t = 2000\text{V/m}$. $B = 0.01\text{T}$. $k=1000\text{m}^{-1}$. $\nu=5\text{MHz}$. $\langle\text{HP}\rangle = 80$.

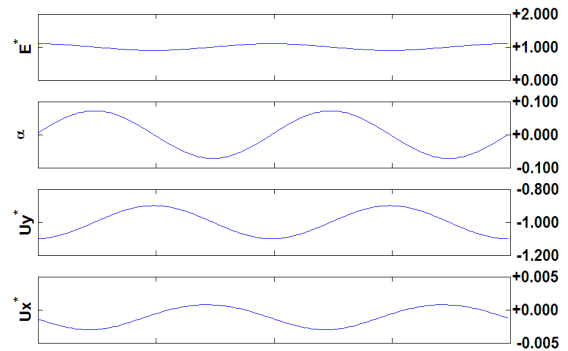


Figure 5. Electron momentum equation's solution for a prescribed electric field. $E_0 = 2000\text{V/m}$. $E_t = 200\text{V/m}$. $B = 0.01\text{T}$. $k=1000\text{m}^{-1}$. $\nu=5\text{MHz}$. $\langle\text{HP}\rangle = 940$.

For a more comprehensive summary of the electron momentum equation and the effect of strong α_{max} , Fig. (6) and Fig. (7) depict the time-averaged Hall parameter for varying choices of frequency and wave number. In some cases, the transport far exceeds classical levels. As before, the classical Hall parameter for all cases is 1000.

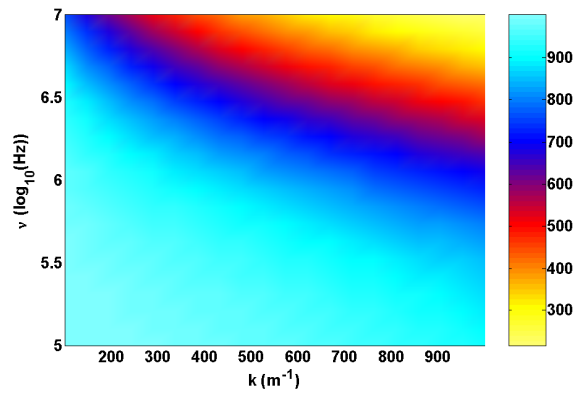


Figure 6. Solution to electron momentum equation for varying k and ω . $E_t = 1000\text{V/m}$. $E_0 = 2000\text{V/m}$. $B=0.01\text{T}$.

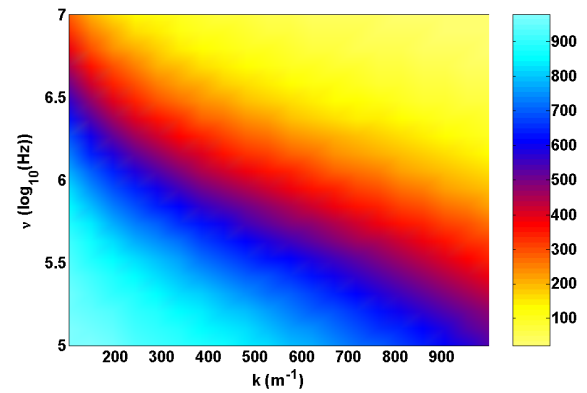


Figure 7. Solution to electron momentum equation for varying k and ω . $E_t = 200\text{V/m}$. $E_0 = 2000\text{V/m}$. $B=0.01\text{T}$.

IV. Impact of Parametric Instability

To qualitatively approximate the potential impact of the beam-plasma instability on electron transport for realistic discharge conditions, a simple model was devised within the constraints of a previously existing 1-D fully periodic fluid model. The electric field was modeled as a raised sinusoidal wave with a peak field and FWHM consistent with the r-z code. On top of this, a 2.5kV/m ripple was imposed with $k=300\text{m}^{-1}$ and $\omega=5\text{MHz}$. The electron-neutral collision frequency was made to decrease uniformly across the solution domain from 10MHz to 1MHz, and the magnetic field was constant at 0.01T. The solution is shown in Fig. (8). The time-averaged hall parameter is shown against the classical hall parameter. Despite the limitations of this model or the r-z code, the beam-plasma instability is capable of effecting a large change in the apparent electron mobility near the exit plane. Near the exit, the Hall parameter including axial fluctuations is comparable to the Bohm approximation – consistent with experimental results³⁻⁴.

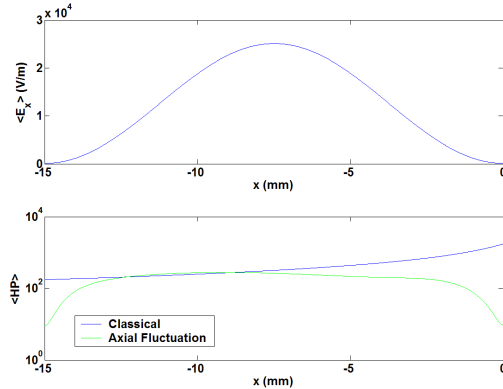


Figure 8. Solution to beam-plasma model.

V. Conclusion

When gradient transport processes in space and time are considered that cause the saturation of axial fluctuations, a beam-plasma parametric instability recently documented in an r-z hybrid code is capable of explaining the anomalous transport near the exit plane of a hall accelerator. The only limitation of this result is that the instability and the induced transport are not modeled in a fully self-consistent manner. The magnitude of the instability is determined by imposing the time-averaged electron mobility into an r-z Hybrid code, and the fluctuations are analyzed separately to see if they are consistent with the observed mobility. In addition, azimuthal fluctuations are not considered, though they are expected to affect the electron mobility, and are expected to have a rather dramatic effect (as per Eq. (26)). Future work will consider the self-consistent axial beam-plasma parametric instability, and the potential impact of azimuthal fluctuations.

VI. Acknowledgements

This research was supported by the Air Force Office of Scientific Research. C. A. Thomas also received support from the National Science Foundation, and from Stanford University, through the Stanford University Graduate Fellowship Program.

VII. References

- ¹D. Bohm, E.H. Burhop, and H.S. Massey. "The Use of Probes for Plasma Exploration in Strong Magnetic Fields", in "The Characteristics of Electrical Discharges in Magnetic Fields." A. Guthrie, R.K. Wakerling, ed. McGraw-Hill (1949).
- ²G.S. Lanes and R.S. Lowder. *Physics of Fluids*, 9, 1115-1123 (1966).
- ³N.B. Meezan, W.A. Hargus, and M.A. Cappelli. *Physical Review E*, 63, 026420 (2001).
- ⁴N.B. Meezan, and M.A. Cappelli. *Physical Review E*, 66, 036401 (2002).
- ⁵E.Y. Choueiri. AIAA-94-3013 (1994).
- ⁶N.B. Meezan, W.A. Hargus, and M.A. Cappelli. "Optical and Electrostatic Characterization of Oscillatory Hall Discharge Behavior" AIAA-1998-3502 (1998).
- ⁷A. Lazurenko, V. Vial, M. Prioul, and A. Bouchoule. *Physics of Plasmas* 12, 013501 (2005).
- ⁸M.K. Allis, N. Gascon, C. Vialard-Goudou, M.A. Cappelli, E. Fernandez. "A Comparison of 2-D Hybrid Hall Thruster Model to Experimental Measurements." Proceedings from the 40th Joint Propulsion Conference (2004).
- ⁹S. Barral, K. Makowski, Z. Peradzynski, and M. Dudeck, "Longitudinal Oscillations in Hall Thrusters", Proceedings of the 4th International Conference on Spacecraft Propulsion, Sardinia (2004).
- ¹⁰N. Gascon, M.K. Allis, C.A. Thomas, and M.A. Cappelli. "A Closer Look at Longitudinal Oscillations inside a Hall thruster." AIAA-2004-3780 (2004).

- ¹¹S. Barral, K. Makowski, Z. Peradzynski, N. Gascon, and M. Dudeck. *Physics of Plasmas*, 10(10), 4137-4152 (2003).
- ¹²K.C. Shaing, A.Y. Aydemir, and R.D. Hazeltine. *Physics of Plasmas*, 5(10) (1998).